EARTH'S CRYOSPHERE
SCIENTIFIC JOURNAL

Earth`s Cryosphere, 2018, vol. XXII, No. 5, pp. 57–66 **http://earthcryosphere.ru/**

METHODS OF CRYOSPHERE'S RESEARCH

DOI: 10.21782/EC2541-9994-2018-5(57-66)

AUDIO-FREQUENCY MAGNETOTELLURIC SURVEYS WITH NON-GROUNDED LINES FOR IMAGING THE RESISTIVITY STRUCTURE OF THE RYBACHIY PENINSULA (MURMANSK REGION)

A.K. Saraev, K.M. Antashchuk, I.S. Eremin

St. Petersburg State University, Institute of Earth Sciences,
7/9, Universitetskaya nab., St. Petersburg, 199034, Russia; a.saraev@spbu.ru

The resistivity structure of the Rybachiy Peninsula (Murmansk region) was studied in winter by audio-frequency magnetotelluric (AMT) surveys using long non-grounded lines and a preamplifier with a high input resistance. The acquired data were processed by robust techniques. Reliable measurements were provided in an audio-frequency range of 7–8 to hundreds of hertz. The results collected in winter with non-grounded lines were no worse than summer measurements with grounded lines. The AMT surveys can resolve the basement top under 5–6 km of low-conductive sediments. The obtained resistivity section of the area represents the transition between the Fennoscandian shield and the Barents shelf and comprises highly permeable water-saturated conductors. The basement depth estimate by inversion of AMT curves was proven valid by subsequent drilling. The AMT surveys have provided updates for the local crust structure inferred from seismic data. The method is applicable to surveys in the Arctic areas of Russia and other permafrost territories.

Audiomagnetotelluric soundings, electric field, non-grounded lines, Rybachiy Peninsula, permafrost

INTRODUCTION

Permafrost is widespread in high latitudes and occupies more than 60 % of the Russian territory. The knowledge of the permafrost structure is indispensable for the development of this territory, construction, and laying railways, roads, and pipelines. Much attention has been given lately to extension of mineral and petroleum exploration into northern areas, where special geophysical instruments are required for surveys on ice and snow during prolonged winter seasons. Magnetotelluric sounding at audio frequencies (AMT survey) ensures fast acquisition of earth responses to excitation by natural sources and can image the subsurface over a large depth span from tens of meters to several kilometers. In this respect, adaptation of AMT survey to permafrost conditions is of high importance.

The reported AMT surveys in the Rybachiy Peninsula, at the transition from the Fennoscandian shield to the Barents shelf, aimed at imaging the resistivity structure of the territory and detecting potential oil and gas reservoirs. The AMT measurements run on snow in winter using snow vehicles to move between stations allow good coverage of the peninsula, which is hardly accessible over its greatest part, and offer an appropriate alternative and extension to the surveys in summer when the use of tracked vehicles is prohibited for environmental reasons. The electrical field was measured with non-grounded capacitive lines. The methods and results of these surveys are the subject of this paper.

AMT METHOD, INSTRUMENTS, AND SOFTWARE FOR DATA PROCESSING AND INTERPRETATION

Audio-frequency magnetotelluric (AMT) survey is a high-frequency modification of magnetotelluric (MT) measurements operated in a range of few to thousands of hertz [*Strangway et al., 1973*]. It measures natural electromagnetic fields [*Berdichevskiy and Dmitriev, 2009; Chave and Jones, 2012*] which are induced by distant lightning storms and propagate around the globe along the Earth-ionosphere waveguide.

The AMT method measures the horizontal components of the electric (E_x, E_y) and magnetic (H_x, H_y) fields. The electric and magnetic field components in a laterally inhomogeneous subsurface are linearly related through the impedance tensor, in a randomly oriented system of *xy* coordinates, as

$$E_x = Z_{xx}H_x + Z_{xy}H_y,$$
$$E_y = Z_{yx}H_x + Z_{yy}H_y,$$

where Z_{xy}, Z_{yx} and Z_{xx}, Z_{yy} are, respectively, off-diagonal (principal) and diagonal (supplementary) components of the impedance tensor.

In laterally homogeneous media, the principal impedance tensor components are equal to the ratios of horizontal and mutually orthogonal electric and magnetic components:

$$Z_{xy} = \frac{E_x}{H_y}, \quad Z_{yx} = -\frac{E_y}{H_x}, \quad Z_{xy} = -Z_{yx}.$$

Calculations for the laterally inhomogeneous case require rotation of the coordinate axes, plotting polar diagrams, and estimating the impedance tensor along the homeogeneity and inhomogeneity axes of the target structure. For 2D inhomogeneities, the tensor components correspond to the E- and H-polarized field (Z^{E}, Z^{H}) and are converted to apparent resistivities (ρ_a) and impedance phases (φ_z):

$$\rho_a^{\mathrm{E}} = \frac{1}{\omega\mu_0}\left|Z^{\mathrm{E}}\right|^2,\ \rho_a^{\mathrm{H}} = \frac{1}{\omega\mu_0}\left|Z^{\mathrm{H}}\right|^2,$$

$$\varphi_z^{\mathrm{E}} = \tan^{-1}\left(\frac{\mathrm{Im}\,Z^{\mathrm{E}}}{\mathrm{Re}\,Z^{\mathrm{E}}}\right),\ \varphi_z^{\mathrm{H}} = \tan^{-1}\left(\frac{\mathrm{Im}\,Z^{\mathrm{H}}}{\mathrm{Re}\,Z^{\mathrm{H}}}\right),$$

where $\omega = 2\pi f$ is the cicrular frequency; f is the working frequency, Hz; $\mu_0 = 4\pi\cdot10^{-7}$ H/m is the magnetic constant.

The frequency dependences of ρ_a and φ_z are AMT curves, which are inverted to the resistivity structure at depths from tens of meters to several kilometers. The AMT data are interpreted with reference to a planar primary incident EM field propagating vertically downward.

The AMT surveys in the Rybachiy Peninsula were performed using the ACF-4M system designed at the St. Petersburg University and the *MicroKOR* company [*Saraev et al., 2011*]. The system consists of a digital recorder, with four synchronous channels and a 24-bit ADC in each channel, electrical receiving lines, and magnetic antennas. The data are acquired in three subranges (0.1–40 Hz, D1; 1–400 Hz, D2; and 1–1000 Hz, D3) of the 0.1 to 1000 Hz range, at sampling rates of 160, 1600 and 3200 Hz, respectively.

The software built into the recorders (SM27) sets up the measurement parameters, runs the measurements automatically, visualizes the acquired data as spectrograms and mutual coherence plots, saves the data and exports them to an external workstation. The data collected in the conditions of noise and low unstable EM fields are processed with the *SM+* software using various robust procedures. Initial and inverted data are visualized with the *Geoinf* software designed for viewing raw MT responses and results of their inversion at specific points along profiles (1D) and in areas (2D).

We applied linearized inversion [*Porokhova and Kharlamov, 1990*] for 1D and *ZondMT2D* (http://zond-geo.com/) and Okkama's inversion for 2D [*de Groot-Hedlin and Constable, 1990*] data. In the latter case, terrain effects were taken into account in inversion of the curves for H- and E-polarized fields and effective curves, as well as for bimodal inversion. The weight of different parameters was variable during the inversion, and *a priori* data could be used for reference.

APPLICABILITY OF NON-GROUNDED LINES TO ELECTRIC FIELD MEASUREMENTS IN THE AMT RANGE

The electric earth responses in conventional AMT surveys are commonly acquired with grounded antennas (receiver electric lines), but the conditions are often unsuitable for grounding (frozen ground, snow and ice in winter or dry sand, rocky and bouldery terrain in summer). There are several approaches to AMT surveys in these conditions, including measurements along three orthogonal components of the magnetic field (one vertical and two horizontal components), as practiced by *Phoenix Geophysics* (Canada) [*Ingerov et al., 2009*]. The three-component measurements of the magnetic field have progressed much lately in terms of theoretical background and methods for data processing and interpretation [*Berdichevskiy and Dmitriev, 2009*]. However, this approach has a pitfall: the vertical magnetic component is zero in a horizontally layered earth (the basic structure in the surveys) and appears only in a laterally inhomogeneous earth. Thus, it is impossible to measure three filed components in this case, and the technique can be only complementary to but not substitutive of impedance measurements applicable to homogeneous and inhomogeneous earth.

We suggest another approach with non-grounded capacitive lines to measure the electric field at audio frequencies. Non-grounded lines were successfully used earlier for radio-frequency measurements (10–1000 kHz) [*Veshev, 1980*] and tested in many field experiments. The method uses (a) symmetrical receiver lines, 100 m of total length, unlike the shorter (40 m) grounded lines; (b) preamplifiers with a high input resistance of R_{in} = 40–200 MOhm, unlike R_{in} = 2 MOhm in the case of grounded lines; (c) robust processing techniques to attenuate noise associated with the operation of a high-resistance preamplifier.

Electric responses of a sufficient strength have to be acquired by receiver lines longer than in the case of grounding. The length of 100 m was chosen experimentally, to ensure sufficiently high signals and the best survey performance.

The preamplifiers with R_{in} = 2 MOhm are optimal for grounded lines, where the transient resistance rarely exceeds 10 kOhm, but have to be operated at higher input resistance when the lines are not grounded and the transient resistance is high. The experimentally found preamplifier input resistance for winter surveys on snow is 40 MOhm. It is not very high though, because the natural electric field at audio wavelengths is lower in winter than in summer, while the higher input resistance causes greater instrumental noise and deteriorates the data quality. High capacitive coupling between the ground and the cable laid on snow is another favorable factor for using pre-

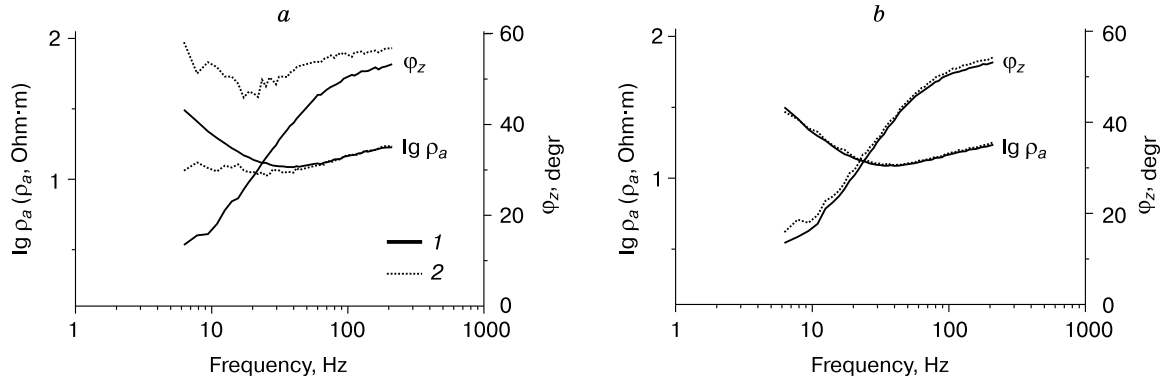

Fig. 1. Apparent resistivity (ρ_a) and impedance phase (φ_z) curves acquired with grounded (*1*) and non-grounded (*2*) lines and preamplifiers with 2 MOhm (*a*) and 40 MOhm (*b*) input resistances.

amplifiers with moderate R_{in} in winter time. Meanwhile, preamplifiers with at least 200 MOhm R_{in} are required for summer surveys, as dry sand and stones fail to provide good ground-cable contact. The high noise of these preamplifiers does not preclude collecting good data because the field itself is higher in summer.

We performed AMT surveys on snow in winter, using non-grounded lines and preamplifiers with input resistances of 2 and 40 MOhm (Fig. 1). The data differ obviously from ρ_a and φ_z curves collected using grounded lines, also in winter (Fig. 1, *a*), in the case of R_{in} = 2 MOhm: at 6–200 Hz for impedance phase and 6–30 Hz for apparent resistivities. With a R_{in} = = 40 MOhm preamplifier, however, the ρ_a curves coincide over the whole range 6–200 Hz, while the φ_z patterns differ slightly below 8 Hz.

Since high-resistance preamplifiers produce instrumental noise, robust techniques are required for data processing, which are provided by the *SM+* software built into the ACF-4M system. The processing cycle includes cutting off spikes, spectral analysis, calibration, selection of frequency spectra, and robust procedures. The 1–1000 Hz range is divided into several subranges, and each curve comprises about 20 points per dial. FFT spectral analysis is applied to each subrange, in which the signal frame passes through the Blackman window and the respective power spectral densities are calculated. The spectral density values obtained by the subsequent robust regression analysis are used to constrain the upper and lower bounds of the impedance tensor components [*Sims et al., 1971*].

This processing ensures improved data quality (Fig. 2). The autospectrum of the initial electric field is free from Schumann resonance peaks which com-

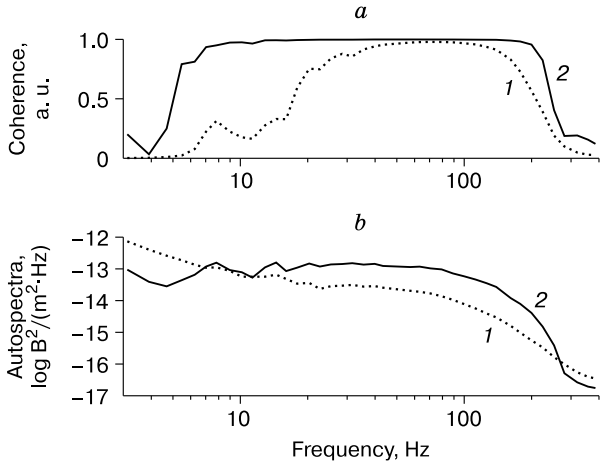

Fig. 2. Autospectra of electric field signals (*b*) and coherence, compared with magnetic field signals (*a*) obtained by processing without (*1*) and with (*2*) robust procedures.

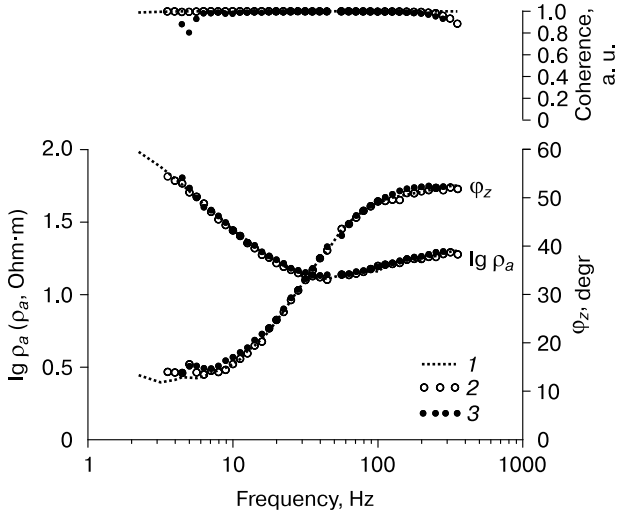

Fig. 3. Apparent resistivity (ρ_a) and impedance phase (φ_z) curves acquired in summer with grounded lines (*1*) and in winter with grounded (*2*) and non-grounded (*3*) lines.

monly appear at 8, 14, 20, 26, 32, ... Hz. The coherence of the electric and magnetic fields is low at 3–30 Hz, indicating considerable influence of incoherent noise on the data, but it exceeds the threshold of 0.9 within 30–150 Hz. The robust processing leads to the presence of peaks at 8 and 14 Hz, which correspond to the Schumann resonance, and the coherence above the threshold at 7–220 Hz.

The quality of winter AMT data collected with non-grounded lines was checked against apparent resistivity and impedance phase curves (Fig. 3) obtained in summer and winter with grounded lines. Surveys with grounded lines yield the best quality data at frequencies from 2.3 to 350 Hz in summer (electric-magnetic field coherence about unity) and at 3.6–350 Hz in winter, when the field is lower. The data acquired in winter with non-grounded lines are of high quality at 6–250 Hz for apparent resistivity and at 8–250 Hz for impedance phase.

The frequency range for non-grounded measurements with the ACF-4M system is limited by the ground-cable capacitive coupling at low frequencies and by the low field level in winter.

RESULTS AND DISCUSSION

The AMT surveys were performed mostly within the Rybachiy Peninsula located in the northern Kola Peninsula (Fig. 4, *A*), as well as in the Sredniy Peninsula and in an isthmus between Rybachiy and Sredniy (Fig. 4, *B*). The local geology consists of Riphean sediments lying over the Archean granitic basement. The sediments include rhythmically alternated conglomerate, sandstone, and siltstone lithologies in the upper section and boulder or boulder-pebble conglomerates and breccias in the lower part, with shales at the section base. The sediments in the Sredniy Peninsula are alternating outsize sandstones in the shallow section part, and siltstone and mudstone below (Fig. 4, *B*).

The two peninsulas are separated by a deep NW tectonic zone along the isthmus. Rocks in the Rybachiy Peninsula form an NW monocline; layers dip generally at 15–35° to the north and northeast and are cut by normal fault planes of different sizes along NW deep faults. In addition to deep faults, there are numerous smaller ruptures striking mainly to the northeast [*Sorokhtin et al., 2011*].

A borehole drilled in the Sredniy Peninsula before the AMT surveys (Pogranichnaya, 5202 m deep, Fig. 4, *B*) stripped the basement at the depth 1175 m. Another borehole (Rybachinskaya) was drilled in the isthmus between the two peninsulas during the AMT surveys (it was 3001 m deep in total, but only ~300 m had been drilled before the surveys).

The surveys were run in winter, with non-grounded lines, along several profiles (see Fig. 4, *B* for

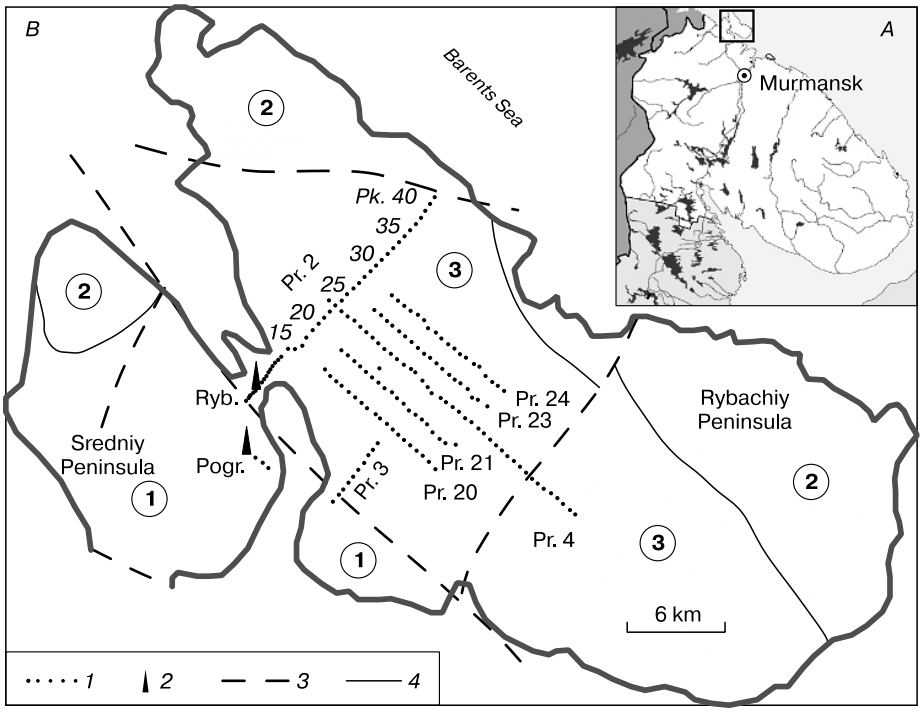

Fig. 4. Location maps of the Kola (*A*) and Rybachiy (*B*) Peninsulas and AMT profiles.

1 – AMT stations along profiles; *2* – Pogranichnaya (Pogr.) and Rybachinskaya (Ryb.) boreholes; *3* – deep faults; *4* – lithology boundaries. Numerals in circles: **1** = outsize sandstones, **2** = interbedded sandstone, siltstone, and mudstone, **3** = sand and conglomerate.

locations). Measurements at each site included recording of horizontal electric and magnetic components along the 40° (E_x and H_x) and 130° (E_y and H_y) directions. Some amount of work was also performed in summer, which confirmed the winter results.

First we processed data along profile 2 (Fig. 4, *B*) running at 40° across the isthmus between Sredniy and Rybachiy as far as the sea shore. Processing yielded pseudosections of apparent resistivity and impedance phase along the profile; polar diagrams of diagonal and off-diagonal impedance tensor components; and directions of structures [*Groom and Bailey, 1989*] at different frequencies.

The obtained data image a 2D structure in the area of profile 2, with mostly NW striking bodies. Although deep faults strike mostly in the NW direction, the field parameters that record the direction of structures are affected by numerous shallow NE faults in the Rybachiy peninsula. Therefore, the Z_{xy} impedance tensor component (azimuth 40°) obtained by processing AMT curves corresponds to the E-polarized transverse electric (TE) mode, while the Z_{yx} component (azimuth 130°) corresponds to the H-polarized transverse magnetic (TM) mode; in previous notations, $Z_{xy} = Z^{E}$, $Z_{yx} = Z^{H}$.

The pseudosections along profile 2 show low ρ_a^{xy} and high φ_z^{xy} within the isthmus between the Sredniy and Rybachiy peninsulas for the E-polarized field (Fig. 5, stations 2–7), but high ρ_a^{yx} and low φ_z^{yx} for the H-polarized field. 3D forward modeling with the *WinGLink* software (*http://www.slb.com*) was applied to find the causes of this difference. One model simulated possible effect of gulfs in the Barents Sea located 1–1.5 km far from the profile (Fig. 4). The model (Fig. 6) represented a two-layer earth (ρ = = 50 000 Ohm·m basement and ρ = 500 Ohm·m sediments, 2 km thick) and two shallow conductors (ρ = 0.5 Ohm·m, 200 m thick) corresponding to the gulfs. According to the modeling results (shown for the y = 10 km profile in the 7–500 Hz range in Fig. 7), the gulfs cause a stronger effect on the apparent resistivity and impedance phase curves of the TE (*XY*) mode. The model pseudosections for the TE mode generally agree with field data (Fig. 5). Therefore,

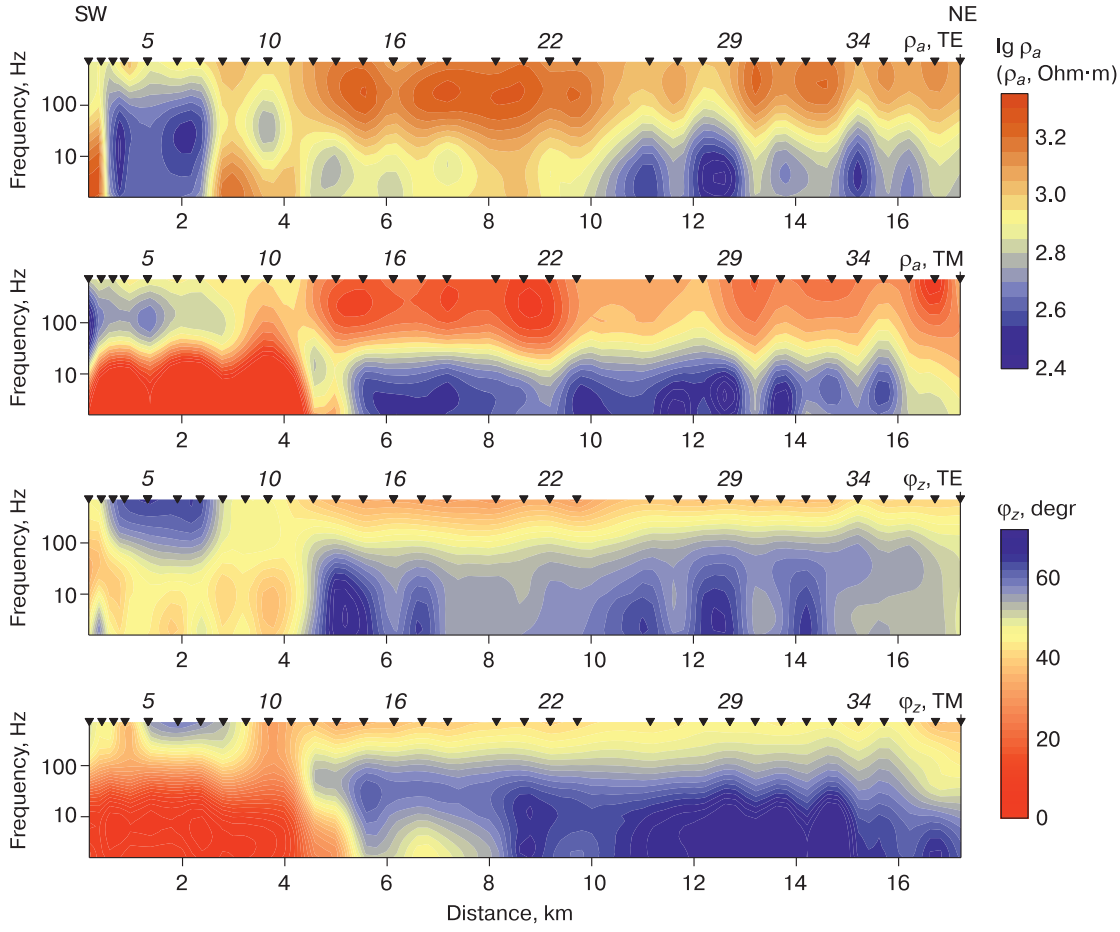

Fig. 5. Pseudosections of apparent resistivity (ρ_a) and impedance phase (φ_z) for TM (*YX*) and TE (*XY*) modes along profile 2.

Black triangles are AMT stations.

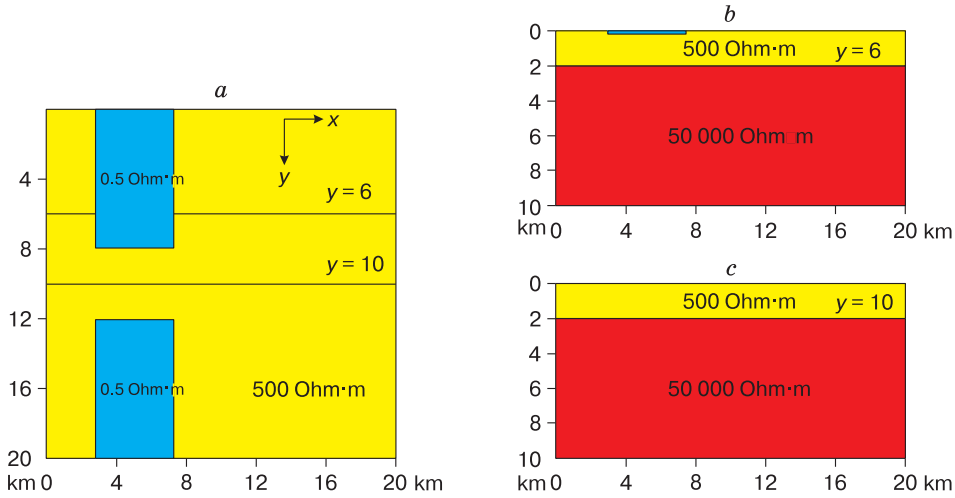

Fig. 6. Model for estimating the effect of sea gulfs on AMT data in the isthmus between the Sredniy and Rybachiy Peninsulas.

a: horizontal plane; *b*, *c*: sections along profiles y = 6 and 10 km.

further inversion was applied to the AMT curves for the TM mode.

The AMTS results were compared with well logs from the Pogranichnaya borehole where the depth to the basement was known (1175 m). The AMT survey was performed at three stations in the borehole vicinity (Fig. 4, *B*) and the curves for the TM mode were inverted in 1D (given the small number of stations) using linearization [*Porokhova and Kharlamov, 1990*].

The resistivity pattern of the borehole site (Fig. 8, *a*) corresponds to the following section structure (top to bottom): 499 m of Riphean sandstone; 280 m of interbedded sandstone, siltstone, and mudstone; 160 m of sandstone; 236 m of interbedded sandstone, siltstone, and mudstone. The sediments are less resistive in the upper 800 m than in the lower 800–1200 m depth interval (100–500 Ohm·m against 500–2000 Ohm·m, respectively). The Archean basement stripped at the depth 1175 m is marked by a high resistivity of >2500–3000 Ohm·m.

The depth to the basement was also estimated by means of linearized inversion of H-polarized (TM-mode) AMT curves within a fragment of profile 2 near Rybachinskaya borehole (Fig. 4, *B*). The resistivity section (Fig. 8, *b*) was obtained with reference to the results for the Pogranichnaya site and the >2500–3000 Ohm·m basement was revealed at a depth of 1400 m. This estimate was proven valid by subsequent drilling (Rybachinskaya borehole) which tapped the basement at 1350 m.

The basic features of the central Rybachiy Peninsula were imaged in impedance phase contour line maps at different frequencies (Fig. 9, *a*, 8, 70, 200 Hz for the H-polarized field). Note that the impedance phase can resolve a deeper earth and is less affected by shallow inhomogeneities. The area in the map for

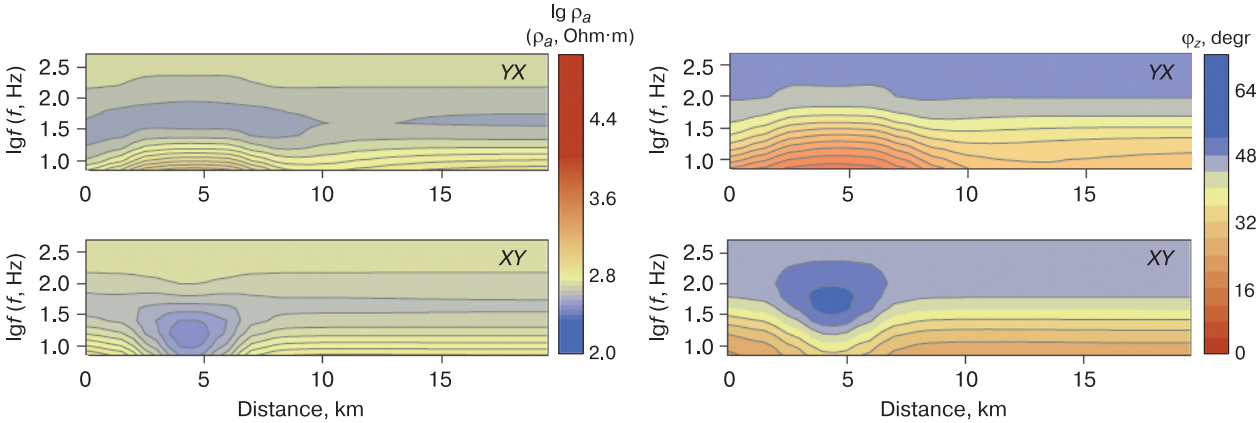

Fig. 7. Results of 3D modeling along profile y = 10 km: apparent resistivity (ρ_a) and impedance phase (φ_z) pseudosections for TM (*YX*) and TE (*XY*) modes (*f* is frequency, Hz).

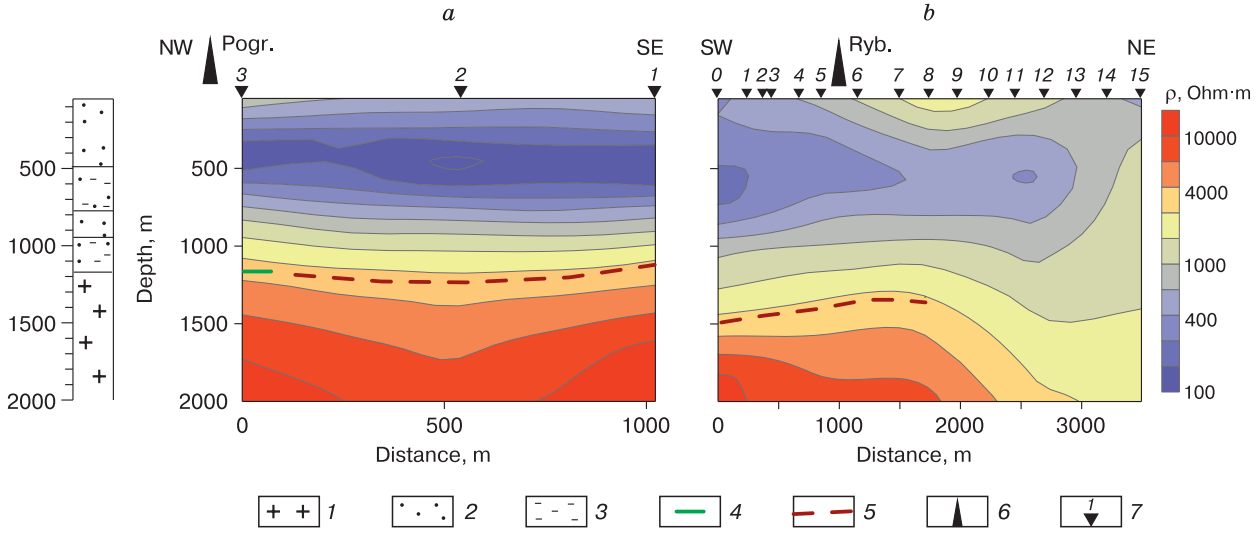

Fig. 8. Resistivity sections obtained by 1D inversion of AMT curves at the Pogranichnaya (*a*) and Rybachinskaya (*b*) drilling sites.

1 – basement granite; *2* – sandstone; *3* – siltstone and mudstone; *4*, *5* – depth to basement according to drilling (*4*) and AMT (*5*) data; *6* – boreholes; *7* – AMT stations and their numbers.

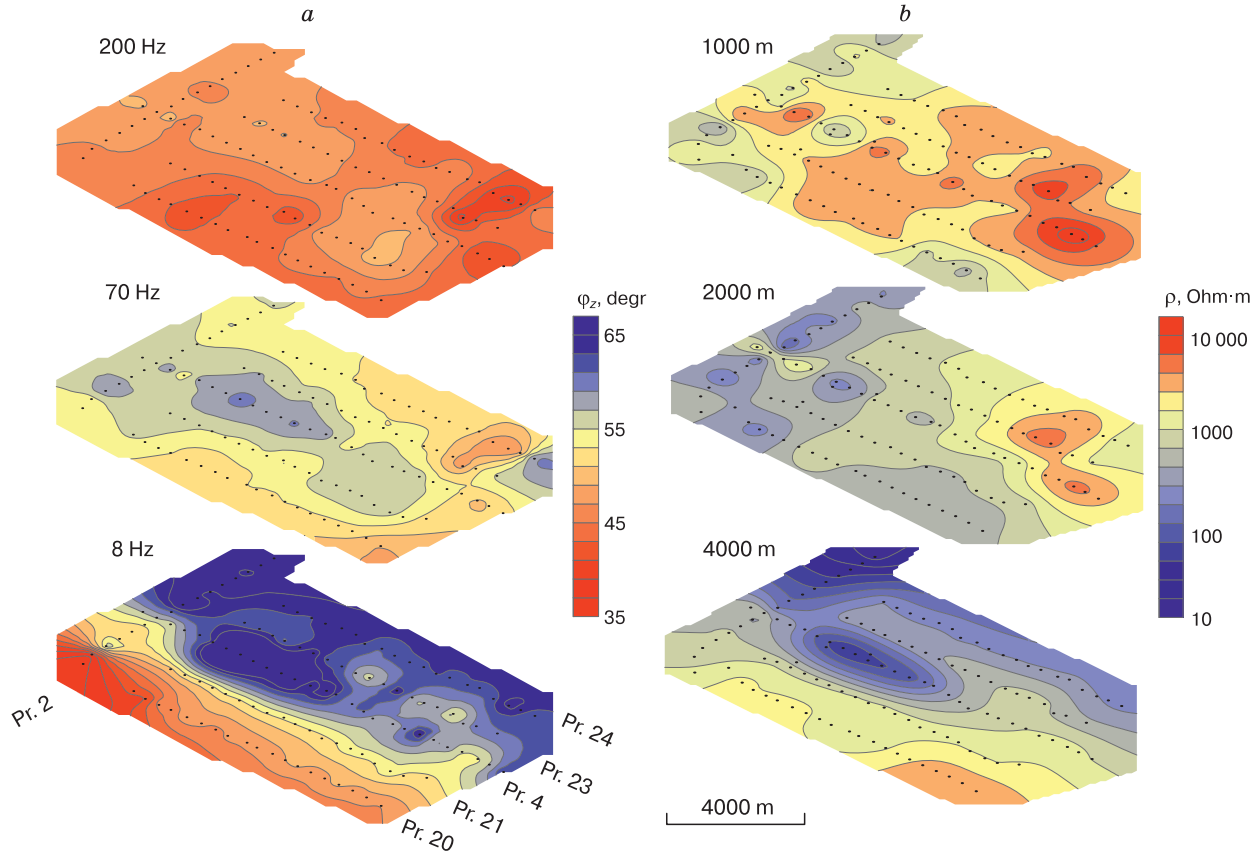

Fig. 9. Contour line maps of impedance phase (φ_z) at different frequencies (*a*) and resistivity (ρ) at different depths (*b*).

Dots are AMT stations.

8 Hz consists of two contrasting zones with an NW boundary. The southwestern part has a low impedance phase (high resistivity typical of the basement), with sharp transition between profiles 4 and 21, possibly, corresponding to a fault in the basement. The northeastern part (profiles 4, 23, and 24) comprises a conductive block at a depth, and the basement is undetectable at 8 Hz.

The map for 70 Hz shows an impedance phase high in the central part of the area, which corresponds to a conductor lying above the basement top. The map for 200 Hz images the shallow section which is more resistive than the conductors appearing at 8 and 70 Hz.

Resistivity patterns at the depths 1000, 2000, and 4000 m in the central Rybachiy Peninsula were mapped based on 2D inversion of AMT curves for the H-polarized field along five profiles (Fig. 9, *b*). The maps resolve well the zones of high and low resistivity at different depths. The conductor in the central part of the area along profile 4 is of special interest in terms of petroleum reservoir potential. The conductor in the 3–4 km depth range may represent permeable water-saturated rocks potentially favorable for oil and gas accumulation.

The 2D resistivity structure, which is less distorted by shallow inhomogeneities, was imaged along profile 2, 19 km of total length (Fig. 4, *B*). Data from a fragment of this profile across Rybachinskaya borehole were inverted in 1D (see above, Fig. 8, *b*). The section obtained by 2D inversion of AMT curves for the H-polarized field (Fig. 10, *a*) comprises three zones separated by deep faults. The southwestern part of the profile (stations 0–13) includes a resistivity high at the depth 1400 m ($\rho < 50\,000$ Ohm·m) corresponding to the basement (see above, Fig. 9, *a*). The second zone (stations 13–23) has a complex structure, with a deep fault and a series of normal faults in the basement, and sediment thickness increasing toward the Barents Sea. The resistivity low between stations 13 and 17 marks the large fault between the Rybachiy and Sredniy peninsulas. The basement is reliably resolved to the depths 5–6 km within the two zones. The third zone (stations 23–45) has a two-layer structure with a heavily faulted upper layer (2–4 km thick; ρ = 500–2000 Ohm·m) and a ρ = 10–100 Ohm·m lower layer within the depth range from 2–4 to 6–8 km. The AMT penetration in this zone is shallower, because of the conductive lower layer, and the basement top is undetectable.

The resistivity structure was also imaged within a CMP reflection profile [*Sharov et al., 2007*] (the profile part covered by AMTS is shown by vertical dashed lines in the seismic section in Fig. 10, *b*). The

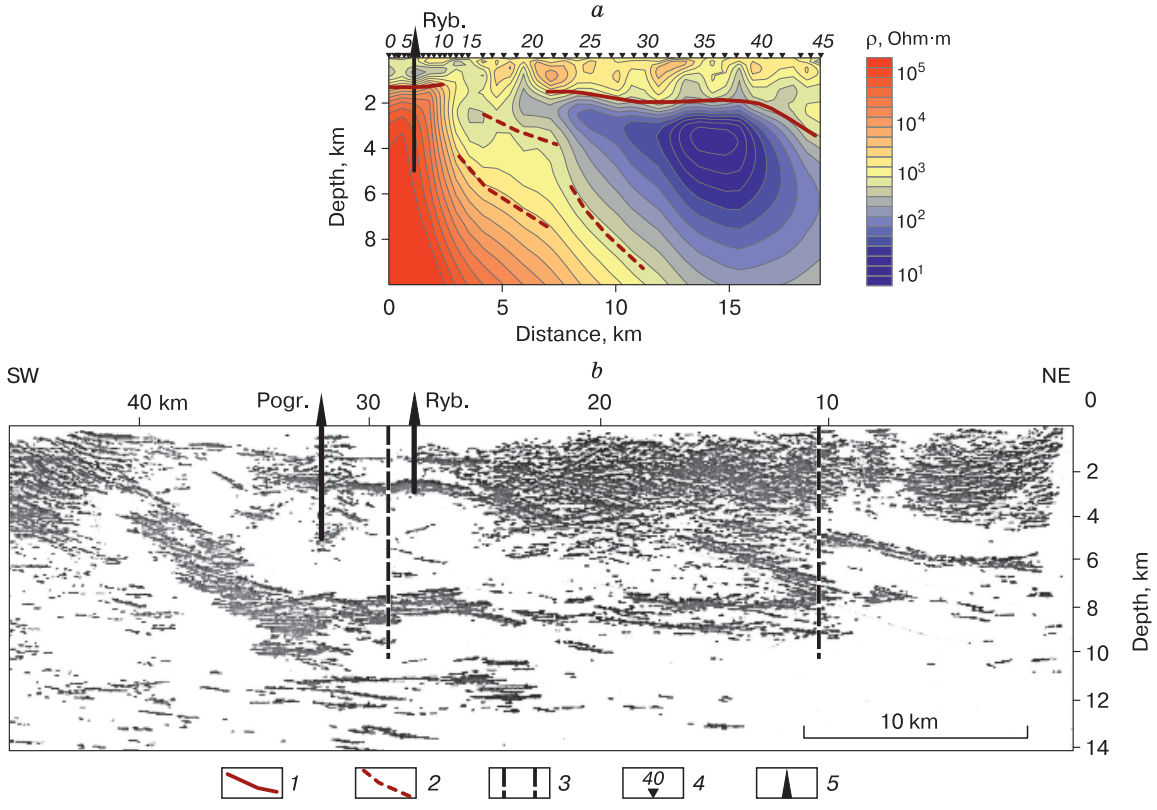

Fig. 10. Resistivity (*a*) and seismic (*b*) sections along profile 2.

1 – reliable boundaries; *2* – inferred boundaries; *3* – seismic profile interval where AMT surveys were performed; *4* – AMT stations and their numbers; *5* – boreholes.

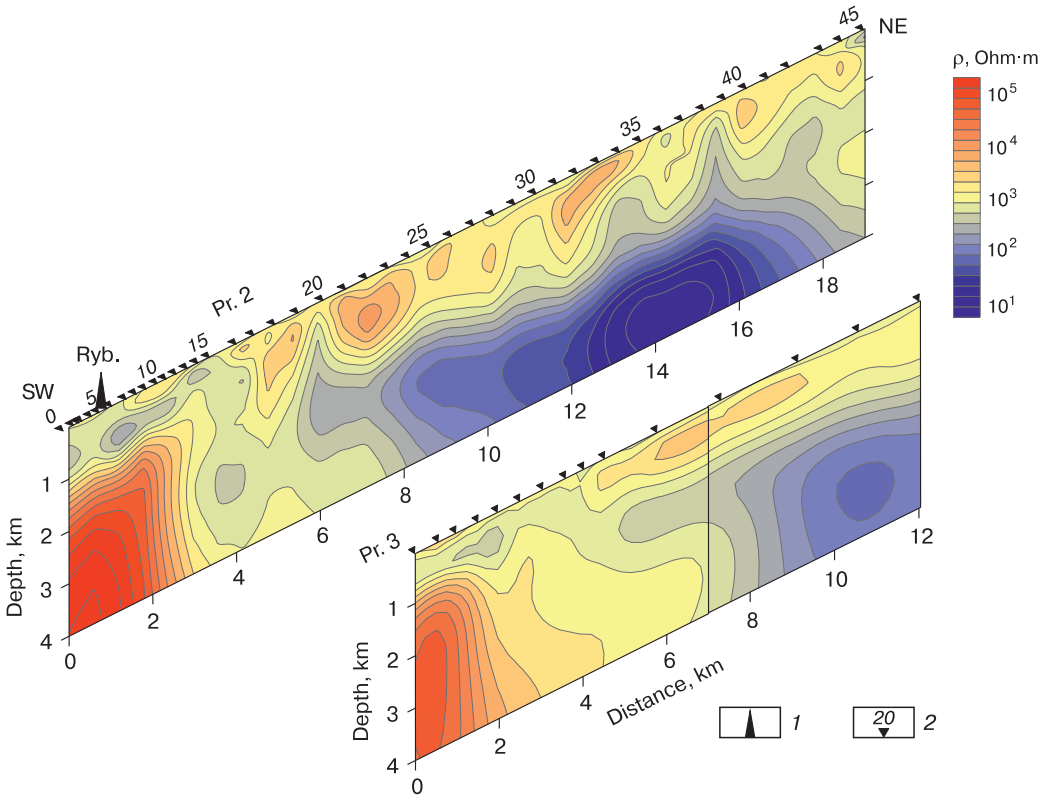

Fig. 11. Resistivity sections along profiles 2 and 3.

1 – boreholes; *2* – AMT stations and their numbers.

previous seismic data were used as a guide for the placement of the Pogranichnaya and Rybachinskaya boreholes, as part of a petroleum exploration project. The basement was expected at a large depth proceeding from seismic data which imaged its top at 8 km. However, the AMTS results predicted a much shallower depth to the basement (1400 m), which turned out to be consistent with drilling results after the AMT survey: the Rybachinskaya borehole reached the basement at 1350 m.

Comparison of the resistivity sections along profiles 2 and 3 (Fig. 11) shows that main features imaged by the former appear in the latter as well (a resistivity high corresponding to the basement in the southwestern part of the profile and a low at a >3 km depth in the northeastern part). Therefore, profile 2 is typical of the central Rybachiy Peninsula and provides a representative image of the transition from the Fennoscandian shield to the Barents Sea.

CONCLUSIONS

The suggested technology of AMT surveys, with data acquired by systems consisting of long non-grounded lines and high-resistance preamplifiers and then processed by robust methods, ensures high-quality results in the frequency range from 7–8 Hz to 400–600 Hz. These results are no worse than those obtained with grounded lines, i.e., the AMT surveys are workable in summer and winter time, to commensurate accuracy and information value. The possibility of running the measurements all year round is especially important for areas of permafrost with a long snow season.

The AMT data collected in winter on snow in the Rybachiy Peninsula and its surroundings are applicable to the estimation of the basement depth within 5–6 km. This depth was predicted to be 1400 m in the isthmus between the Sredniy and Rybachiy peninsulas, and the estimate was proven valid by later drilling (Rybachinskaya borehole) which tapped the basement at 1350 m. Prior to the AMT surveys, the sediment thickness was expected to be large proceeding from inversion of seismic data that gave a depth of 8 km. Thus, the AMT surveys allowed updates to the previous information.

The resistivity sections obtained by inversion of AMT data image the complex heavily faulted structure of the transition between the Fennoscandian shield and the Barents Sea, with a series of normal faults and a sediment thickness increasing toward the Barents Sea. The structure includes highly permeable

saturated zones where the conditions may be favorable for oil and gas accumulation.

The study was supported by the Geomodel *Resource Center of the St. Petersburg State University.*

References

Berdichevskiy, M.N., Dmitriev, V.I., 2009. Models and Methods of Magnetotelluric Soundings. Nauchnyi Mir, Moscow, 673 pp. (in Russian)

Chave, A.D., Jones, A.G. (Eds.), 2012. The Magnetotelluric Method. Theory and Practice. Cambridge Univ. Press, Cambridge, UK, 552 pp.

de Groot-Hedlin, C., Constable, S., 1990. Occama's inversion to generate smooth, two dimensional models from magnetotelluric data. Geophysics 55 (12), 1613–1624.

Groom, R.W., Bailey, R.C., 1989. Decomposition of magnetotelluric impedance tensors in the presence of local three-dimensional galvanic distortion. J. Geophys. Res. 94, 1913–1925.

Ingerov, O.I, Fox, L., Golyashov, A., Colln, A., 2009. Non-grounded surface electroprospecting technique. 71st EAGE Conference & Exhibition (8–11 June 2009). Amsterdam, Netherlands, p. 251.

Porokhova, L.N., Kharlamov, M.M., 1990. The solution of the one-dimensional inverse problem for induction soundings by an efficient linearization technique. Phys. Earth Planet. Inter. 60, 68–79.

Saraev, A.K., Antashchuk, K.M., Pertel, M.I., Eremin, I.S., Golovenko, V.B., Larionov, K.A., 2011. The ACF-4M system for audio-frequency magnetotelluric surveys, in: Proc. 5th M.N. Berdichevsky and L.L. Vanyan Seminar on Electromagnetic Soundings of the Earth EMS–2011. St. Petersburg University, St. Petersburg, Vol. 2, pp. 475–478.

Sharov, N.V., Isanina, E.V., Krupnova, N.A., Glaznev, V.N., Chikirev, I.V., 2007. Improving the reliability of geological models for the crust of the Sredniy–Rybachiy Peninsulas by joint interpretation of seismic CMP, DSS, and magnetic surveys. Ural Geophys. Vestn., No. 4 (13), 98–106.

Sims, W.E., Bostick, F.X., Smith, H.W., 1971. The estimation of magnetotelluric impedance tensor elements from measured data. Geophysics 36, 938–942.

Sorokhtin, I.O., Kozlov, P.E., Kulikov, H.B., Pozhilenko, V.I., Stupak, V.M., 2011. The evolution of the northwestern Timan-Varangerch oil and gas basin. Bull. Kola Science Center, No. 3, 3–21.

Strangway, D.W., Swift, C.M., Holmer, R.C., 1973. The application of audio-frequency magnetotelluric (AMT) to mineral exploration. Geophysics 38, 1159–1175.

Veshev, A.V., 1980. DC and AC Electro Profiling Surveys. Second Edition. Nedra, Leningrad, 391 pp. (in Russian)

Received June 19, 2017